総合研究報告

# Bi-based Superconductors Fabricated in High Magnetic Fields

Xiaoye LU**

**Abstract**

The microstructure and superconducting properties of Bi-2223 superconductor fabricated in high magnetic fields were systematically investigated. The results shows that the Bi-2212 grains with their *c*-axis parallel to the magnetic field were formed after the partial-melting and solidification in 8 T magnetic field, and transformed into the Bi-2223 grains with *c*-axis alignment during the further sintering process at 840℃ without magnetic field. The conversion of Bi-2212 grains to Bi-2223 grains has the heredity in grain alignment. The mixed structures of the Bi-2223 and the Bi-2212 grains with their *c*-axis parallel to the magnetic field are formed in samples sintered at 850℃- 855℃ in 10 T magnetic field. Below 845℃ sintering in 10 T, a high proportion of Bi-2223 phase is obtained, however no preferred orientation is observed. The Bi-2223 grains with their *c*-axis parallel to the axial direction of the vertical tube furnace are formed not only on the surface, but also in the center of the sample sintered at 850℃ for 120 h in a 15℃/cm temperature gradient without magnetic field. Moreover, the samples sintered in the temperature gradient and in a 10 T magnetic field have a stronger *c*-axis alignment of Bi-2223 phase.

.

## 1. Introduction

In the Bi-Sr-Ca-Cu-O system, three superconducting phases are known to exist. Their compositions can be described by the general formula $Bi_2Sr_2Ca_{n-1}Cu_nO_x$ (n= 1, 2, or 3), where n represents the number of $CuO_2$ planes. They are commonly referred to as Bi-2201 phase for n=1, Bi-2212 phase for n = 2 and Bi-2223 phase for n = 3, and their corresponding critical transition temperatures ($T_c$) are about 20 K, 80 K and 110 K, respectively [(1)]. These phases have structural similarities and can be considered as perovskite-type cells with lattice parameters $a \fallingdotseq b$ =5.4Å stacking up along the *c*-axis with $c_{2201}$=24.5Å, $c_{2212}$=30.8Å, and $c_{2223}$= 37.0Å, respectively. Among all the high-temperature superconductors discovered to date, Bi-2223 phase is the most promising material for tapes and wires for large-scale and high-current applications.

For fundamental research, the growth of larger and more perfect single crystals is important, because it will lead to a better understanding of crystalline materials. Single crystals of superconductors have at present no technical applications, in contrast to the situation in semiconductors, but are essential for the understanding of superconductivity. The growth of large, single-phase crystals of bismuth cuprate phases is very difficult [(2)]. The reason for this can be found in the similar crystallographic structures of the various compounds (which form intergrowths with one another) in the very pronounced tendency to grow in sheets in the *a-b* plane, and in the complicated phase diagrams of these systems. The quaternary system of $B_2O_3$-SrO-CaO-CuO contains 19 known phases [(3)]. The microstructure of Bi-based oxide superconductors consists of plate-like grains with the *a-b* plane along the flat surface of the platelets. If the grains are aligned by stacking the platelets like a structure of bricks [(4)], a high $J_c$ can be achieved in the *a-b* plane. A possible texturing technique which has been frequently used to now is based on crystal growing in a liquid phase subjected to a magnetic field [(5)~(7)] by a procedure known as magnetic melt texturing (MMT).

Mikelson *et al.* [(8)] explained alignment of a magnetic material placed in a magnetic field by following mechanism. The orienting force resulting from the effects of a homogeneous magnetic field acting on a crystal whose paramagnetic susceptibility χ differs along two mutually perpendicular crystallographic axes by a factor Δχ is proportional to $\Delta\chi H_a^2 V \sin 2\Theta$ where Θ is the angle between the direction of the applied magnetic field Ha and the crystallographic axis along which |χ|

**Cooperative Major in Life Cycle Design Engineering, Graduate School of Engineering and Resource Science, Akita University,

is a maximum, and $V$ is the volume of the crystal. Thus a crystal with an anisotropic paramagnetic susceptibility will align with the axis along which $\chi$ has a maximum value parallel to the applied field.

In previous works [(9), (10)], we reported the grain alignment and critical current densities of (Bi,Pb)-2223 phase in the partial-melting and sintering process without magnetic field. However, the grain alignment of the partial-melted samples exists only in their surface layers. In this paper, we systematically study the microstructure and superconducting properties of Bi-2223 superconductors fabricated in high magnetic fields [(11)~(19)].

## 2. Experimental

High purity $Bi_2O_3$, PbO, $SrCO_3$, $CaCO_3$ and CuO powders (99.99% in purity) were weighed and mixed in the atomic ratio Bi:Pb:Sr:Ca:Cu = 1.8:0.4:1.9:2.1:3.5, which is the optimum composition for preparation of Bi-2223 phase in the partial-melting and sintering process [(9)]. After being calcined at 800℃ for 12 h and pulverized, samples were pressed to pellets of 10 mm in diameter and 10 mm thickness by application of an uniaxial pressure of 1.2GPa. The pellets were contained in silver crucibles and heat-treated in a vertical tube furnace installed in a solenoid-type superconducting magnet with a room temperature clear bore 50 mm in diameter [(20)]. A vertical magnetic field ($H_a$) can be applied parallel to the long axis of the furnace.

For the samples of Bi-2223 superconductors formed after partial-melting and solidification, the heat treatment employed is shown in Fig.1. Different maximum temperatures ($T_{max}$), from 870 to 880℃, and different cooling rates ($C_r$), from 0.5 to 5℃/h, have been investigated. All the partial-melting and solidification treatments were carried out in 0 or 8 T magnetic field in air. After the partial-melting and solidification, the samples were sintered at 840℃ for 240 h without magnetic field in air.

For the samples of Bi-2223 superconductors formed in a temperature gradient, the pellets set on a silver holder were sintered at 850℃ for 120 h in a vertical tube furnace with a temperature gradient of 15℃/cm installed in a solenoid-type superconducting magnet. Fig.2 is the temperature distribution measured along the furnace center-line at a 870℃ control temperature. The temperature gradient was about 15℃/cm at the position of -7.5cm (850℃) where the center of the sample was fixed.

The samples were analyzed by XRD. To prevent the surface texture, the samples were cut more than 2 mm in depth from the surface for XRD by a diffractometer (XR-3A) with Cu$K\alpha$ radiation. Microstructure observation was performed by SEM on polished cutting surfaces with EDS. $T_c$ was measured by AC magnetic susceptibility and magnetic hysteresis cycles from 20 to 77 K in fields up to 1 T were measured by a vibrating sample magnetometer (VSM). The degree of texturing of Bi-2223 grains in this study is quantified by an alignment factor $f_{2223}$ defined as

$$f_{2223} = (P - P_o)/(1 - P_o) \quad (1)$$

$$P = H(00\underline{10})/(H(00\underline{10}) + H(115)) \quad (2)$$

where $P$ is a parameter as stated above in the textured sample and $P_o$ is an equivalent parameter for random samples. H(00$\underline{10}$) and H(115) are the integrals of the (00$\underline{10}$) and (115) peaks of Bi-2223 phase, respectively. The volume fraction ($Q_{2223}$) of Bi-2223 phase is defined as

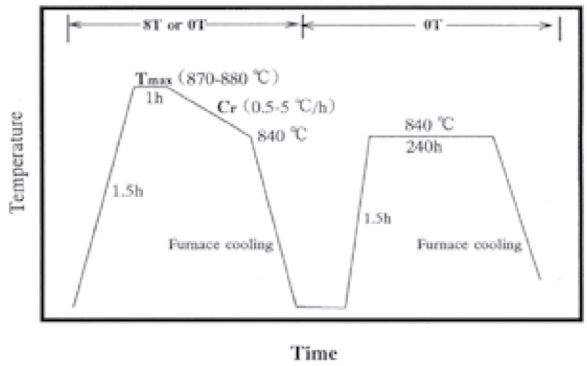


Fig.1 Temperature profile for partial-melting, solidification, and sintering process of the Bi-2223 bulk ceramics.

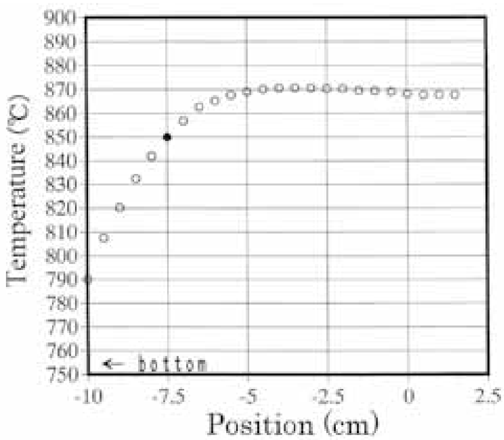


Fig.2 Temperature distribution measured along the furnace center-line at 870℃ control temperature.

$$Q_{2223} = \mathrm{H}(00\underline{10})/(\mathrm{H}(00\underline{10}) + \mathrm{L}(008)) \quad (3)$$

where H(00$\underline{10}$) is the integrals of the (00$\underline{10}$) peak of Bi-2223 phase, and L(008) is the integral of the (008) peak of Bi-2212 phase.

## 3. Results and discussion

### 3.1. Formation of Bi-2223 superconductors after partial-melting and solidification

Figure 3 shows the susceptibility versus temperature plots of samples sintered at 840℃ for 240 h (Samples C and D) after partial-melting at 875℃ and solidification at a cooling rate 2℃/h (Samples A and B). An 8 T field was applied to Samples B and D, while no field was applied to Samples A and C. It is seen that the changes in susceptibility occur at about 85 K due to the diamagnetic property of Bi-2212 phase in Samples A and B which were processed by the partial-melting and solidification. On the other hand, for samples sintered at 840℃ for 240 h (Samples C and D) after partial-melting and solidification, the changes in susceptibility at 108 K due to Bi-2223 phase are observed. And the application of 8 T field has no influence on $T_c$ and the transition width.

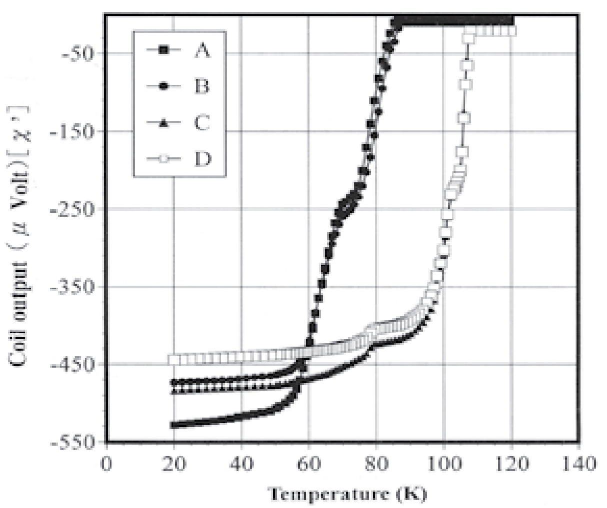


Fig.3 Temperature dependence of AC susceptibility for the samples processed with $T_{max}$=875℃ and $C_r$=2℃/h.
Sample A: processed by partial-melting and solidification in 0T,
Sample B: processed by partial-melting and solidification in 8T,
Sample C: sintered at 840℃ for 240 h for Sample A,
Sample D: sintered at 840℃ for 240 h for Sample B.

Figure 4 shows the XRD patterns of the face oriented perpendicular to the applied field ($H_a$). Its $T_{max}$ and $C_r$ in the preparation temperature profile (Fig.1) are 875℃ and 2℃/h, respectively. (00*l*) peaks are by far the most intense which indicates a strong alignment of the *c*-axis, along the magnetic field direction. The Bi-2212 grains with their *c*-axis parallel to the magnetic field are formed after the partial-melting and solidification in 8 T magnetic field, and transform into the Bi-2223 grains with *c*-axis alignment during the further sintering process at 840℃ without magnetic field.

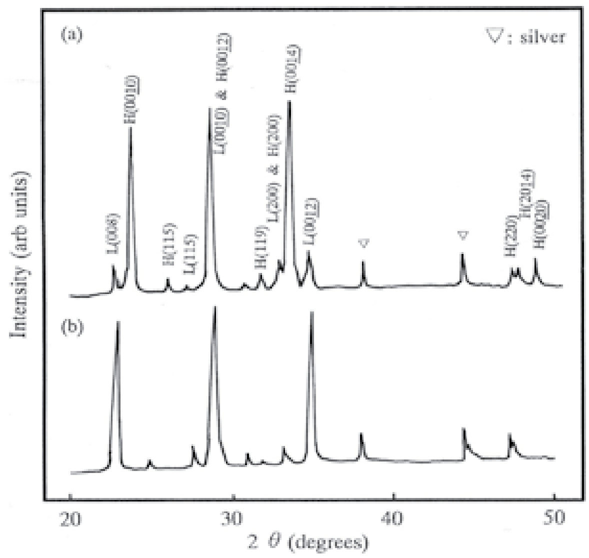


Fig.4 XRD patterns recorded from the horizontal cross-section of (a) a sample sintered at 840℃ for 240 h after partial-melting and solidification in 8T; (b) a sample processed by partial-melting and solidification in 8 T.

Figure 5 show the XRD patterns for the sample prepared using exactly the same heat treatment as shown in Fig.4, but without magnetic field. Although the Bi-2212 grains are formed after the partial-melting and solidification, and transform into the Bi-2223 grains during the further sintering process at 840℃, no anisotropy is observed.

From Figs.4 and 5, it may be concluded that the conversion of Bi-2212 grains to Bi-2223 grains has the heredity in grain alignment. The Bi-2223 grains transformed from the Bi-2212 grains with the alignment will still be aligned, which is consistent with our previous report [10]. On the other hand, this confirms that the magnetic field induces the orientation during solidification.

Both the maximum temperatures ($T_{max}$) and cooling rates ($C_r$) in the temperature profile as shown Fig.1 are found to have obvious influence on the alignment factor $f_{2223}$. The optimum $T_{max}$, from 870 to 880℃, is 875℃ and the optimum $C_r$, from 0.5 to 5℃/h, is 2℃/h. In addition, it should be pointed out that in our experiments, even at a very slow cooling rate of 0.5℃/h during solidification, the Bi-2223 phase cannot be formed directly from the solidification process.

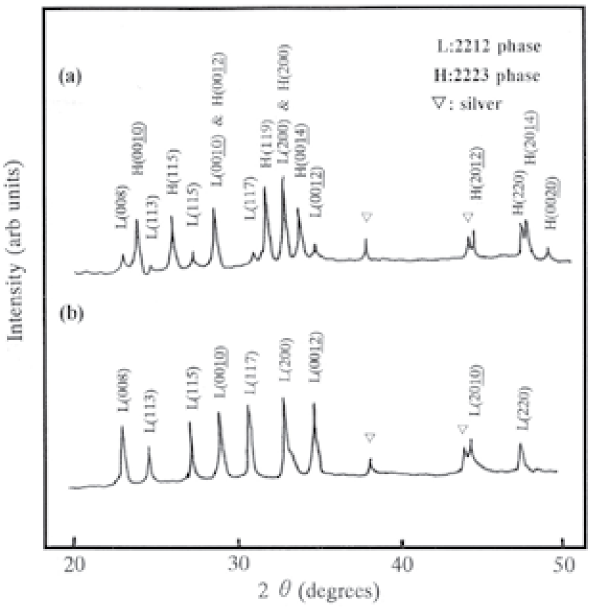


Fig.5 XRD patterns recorded from the horizontal cross-section of (a) a sample sintered at 840℃ for 240 h after partial-melting and solidification in 0 T; (b) a sample prepared by partial-melting and solidification in 0 T.

In order to correlate the texture to the magnetic anisotropy, magnetic hysteresis cycles were measured with measuring magnetic fields parallel or perpendicular to the direction of $H_a$. For the samples prepared without magnetic field, the vertical direction is treated as the direction of $H_a$. Figures 6 and 7 show the measuring results obtained at 20 K for two samples prepared by partial-melting and solidification in 0 and 8 T magnetic fields, respectively. The magnetic hysteresis is almost the same for the sample prepared without magnetic field in two measuring directions. Whereas for the sample processed in 8 T, the hysteresis in the magnetization is greater for a measuring field applied parallel to the direction of $H_a$, that is $\Delta M_{Hm//Ha} > \Delta M_{Hm \perp Ha}$, indicating that for this sample an obvious anisotropy exists and the Bi-2212 grains align with their *c* axes parallel to $H_a$. These results are in agreement with the observation made by other group [21].

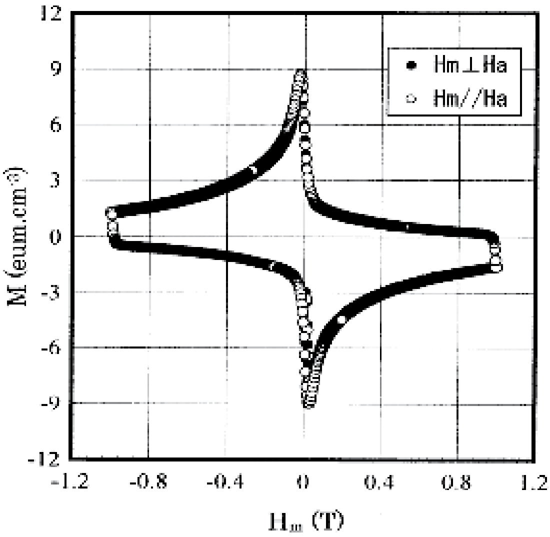


Fig.6 Magnetic hysteresis loops at 20 K for the sample prepared by partial-melting at 875 ℃ and solidification at a cooling rate of 2℃/h without magnetic field.

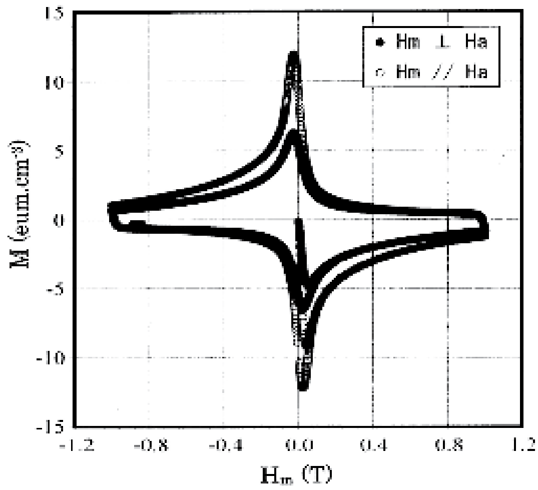


Fig.7 Magnetic hysteresis loops at 20 K for the sample prepared by partial-melting at 875℃ and solidification at a cooling rate of 2℃/h in 8 T magnetic field.

Figure 8 shows the magnetic hysteresis results obtained at 77 K for the sample sintered at 840℃ for 240 h after partial-melting at 875℃ and solidification with the application of an 8 T magnetic field. An obvious anisotropy exists and the Bi-2223 grains align with their *c* axes parallel to $H_a$. The anisotropy observed in the hysteresis measurement is obviously the result of texture development by the application of an 8 T magnetic field during solidification.

The samples' microscopic structure was observed by SEM on polished cutting faces oriented parallel to the applied field ($H_a$). For samples processed without magnetic field, the faces were cut parallel to the direction of axis of the furnace. Figure 9 shows SEM micrographs of the samples sintered at 840℃ for 240 h after partial-melting and solidification in 0 T and 8 T magnetic fields, respectively. Its $T_{max}$ and $C_r$ in the temperature profile ( Fig.1 ) are 875℃ and 2℃/h, respectively. No preferred

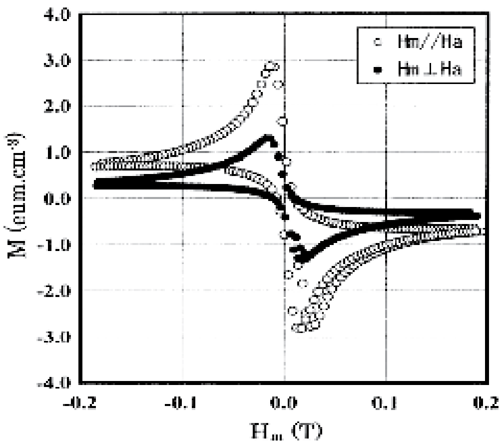


Fig.8 Magnetic hysteresis loops at 77 K for the sample sintered at 840℃ for 240 h after partial-melting at 875℃ and solidification at a cooling rate of 2℃/h in 8 T magnetic field.

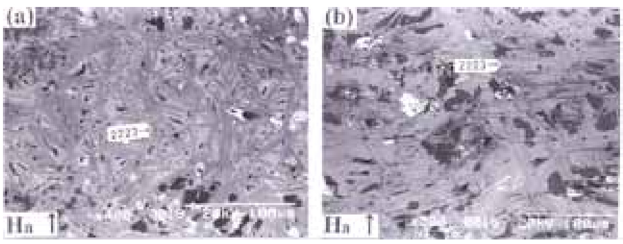


Fig.9 SEM micrographs taken from vertical cross-section of samples sintered at 840℃ for 240 h after partial-melting at 875℃ and solidification at a cooling rate of 2℃/h without magnetic field (a), and with the application of an 8 T magnetic field (b).

orientation is observed in the sample processed without magnetic field (Fig.9a). In contrast, the Bi-2223 platelets are preferentially oriented perpendicular to the processing magnetic field direction in the sample processed in 8 T magnetic field (Fig.9b). This is in agreement with the results of X-ray analysis and magnetic hysteresis measurement.

**3.2. Formation of Bi-2223 superconductors during sintering**

Figure 10 shows the temperature dependence of the susceptibility for samples sintered directly at the temperatures of 840℃, 850℃, 855℃ and 860℃ for 120 h in a 10 T magnetic field, respectively. It can be seen that the susceptibility changes at 82 K due to the Bi-2212 phase for the sample sintered at 860℃ in one step. On the other hand, for the samples sintered at the temperatures below 860℃, the changes in susceptibility occur in two steps. One change at 82 K is due to the diamagnetic property of the Bi-2212 phase and the other change at 108 K is due to the diamagnetic property of the Bi-2223 phase. However, the diamagnetic strength of the Bi-2223 phase is very sensitive to the sintering temperature and the highest diamagnetic strength of the Bi-2223 phase exists in the sample sintered at 840℃.

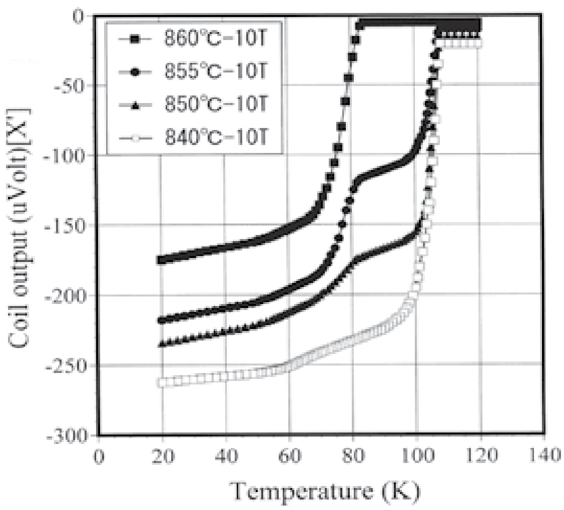


Fig.10 Temperature dependence of the susceptibility for samples sintered at the temperatures of 840℃- 860℃ for 120h in 10T magnetic field.

Figure 11 shows X-ray diffraction patterns recorded from the horizontal cross-section of samples sintered at the temperatures of 840℃, 850℃ and 860℃ for 120 h in a 10 T magnetic field, respectively. For the sample sintered at 860℃, almost all peaks can be identified as Bi-2212 peaks and (00*l*) peaks are by far the most intense which indicates a strong alignment of the *c*-axis, along the magnetic field direction. This indicates the Bi-2212 phase with *c*-axis parallel to the magnetic field are formed in the 860℃ sintering process in 10 T magnetic field. For the sample sintered at 850℃, the mixed structures of the Bi-2223 and the Bi-2212 grains with their *c*-axis parallel to the magnetic field are formed. In the 840℃ sintering, a high proportion of the Bi-2223 phase is obtained, however no preferred orientation is observed.

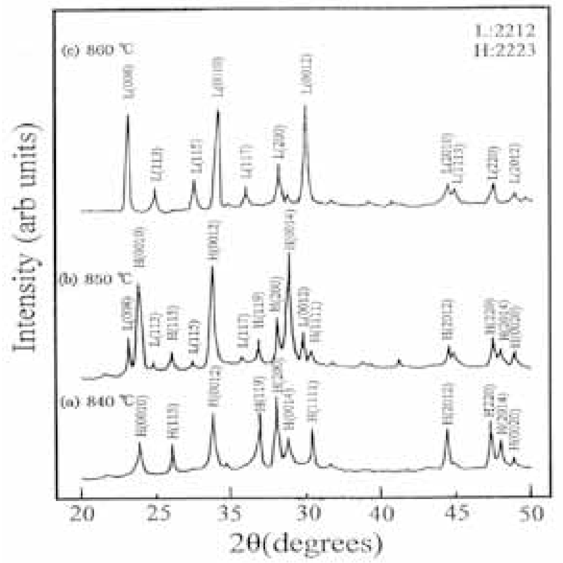


Fig.11 XRD patterns recorded from the horizontal cross-section of samples sintered at the temperatures of 840℃ (a), 850℃ (b) and 860℃ (c) for 120 h in 10 T magnetic field.

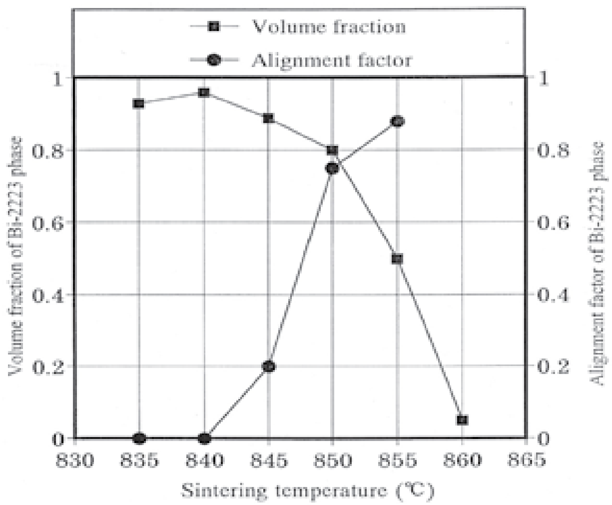


Fig.12 Sintering temperature dependence of the volume fraction and alignment factor of the Bi-2223 phase during sintering in 10 T magnetic field.

Figure 12 expresses sintering temperature dependence of the volume fraction and alignment factor of the Bi-2223 phase during sintering in a 10 T magnetic field. It can be seen that the volume fraction and alignment factor of the Bi-2223 phase are very sensitive to the sintering temperature. With increasing the sintering temperature from 840℃ to 855℃, the alignment factor of the Bi-2223 phase increases, however, the volume fraction of the Bi-2223 phase decreases. In the 850℃-855℃ sintering, the Bi-2223 phase with *c*-axis alignment is formed. Below 845℃ sintering, a high proportion of Bi-2223 phase with a zero alignment factor is obtained. It is suggested that a liquid phase is important for the formation of the textured structure in magnetic fields.

Figure 13 shows SEM micrographs of the samples sintered at the temperatures of 840℃, 850℃, 855℃ and 860℃ for 120 h in a 10 T magnetic field, respectively. According to the analyses by XRD and EDS, the microstructures in these samples mainly consist of Bi-2212, Bi-2223 and Bi-free phase (including $(Sr,Ca)_2CuO_3$ and $(Sr,Ca)CuO_2$). No preferred orientation is observed in the sample sintered at 840℃ (Fig.13a). In contrast, the Bi-2223 and Bi-2212 platelets are preferentially oriented perpendicular to the processing magnetic field direction in samples sintered at 850℃(Fig.13b), 855℃ (Fig.13c) and 860℃ (Fig.13d).

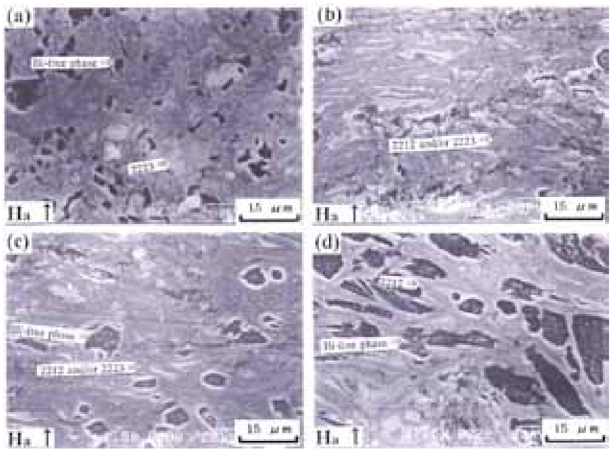


Fig.13 SEM micrographs of the samples sintered at the temperatures of 840℃ (a), 850℃ (b), 855℃ (c) and 860℃ (d) for 120 h in 10 T magnetic field.

Figures 14 and 15 show the measurement results obtained at 77 K for two samples sintered at 850℃ in 0 T and 10 T magnetic fields, respectively. The magnetic hysteresis loops in the two measuring directions are almost the same for the sample prepared without magnetic field. Whereas for the sample sintered in 10 T, the hysteresis in the magnetization is greater for a measuring field applied parallel to the direction of $H_a$, that is $\Delta M_{Hm//Ha} > \Delta M_{Hm\perp Ha}$, indicating that for this sample an obvious anisotropy exists and the Bi-2223 grains align with their *c*-axes parallel to $H_a$. This is consistent with the results of X-ray analysis and SEM observations.

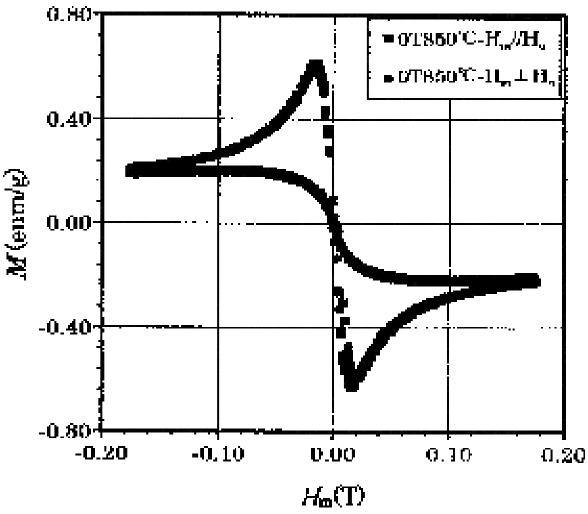


Fig.14 Magnetic hysteresis loops at 77 K for the sample sintered at 850℃ in 0 T magnetic field.

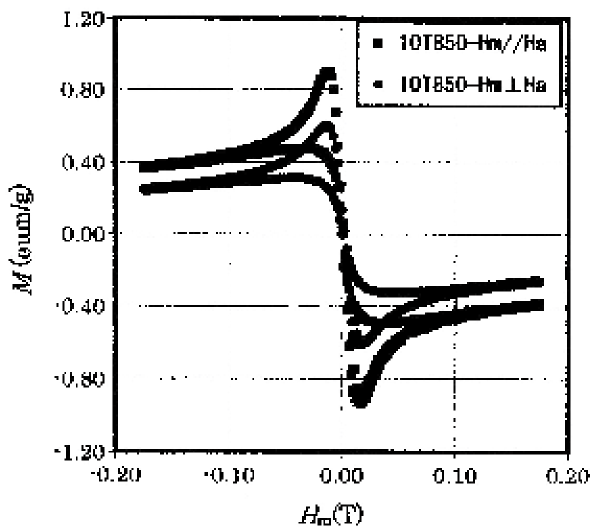


Fig.15 Magnetic hysteresis loops at 77 K for the sample sintered at 850℃ in 10 T magnetic field.

### 3.3. Formation of Bi-2223 superconductors in a temperature gradient

Figure 16 shows X-ray diffraction patterns recorded from the horizontal cross-section at different positions (the upper, center and lower) of the sample sintered at 850℃ for 120 h in 15℃/cm temperature gradient without magnetic field. For the upper horizontal cross-section (Fig.16a), Bi-2212 phase is a major phase and (00*l*) peaks of Bi-2212 phase are by far the most intense which indicates a strong alignment of the *c*-axis, along the vertical direction. For the center horizontal cross-section (Fig.16b), the Bi-2223 phase with *c*-axis alignment as a major phase coexists with minority Bi-2212 phase. For the lower horizontal cross-section (Fig.16c), almost all peaks can be identified as Bi-2223 peaks, however, no preferred orientation is observed.

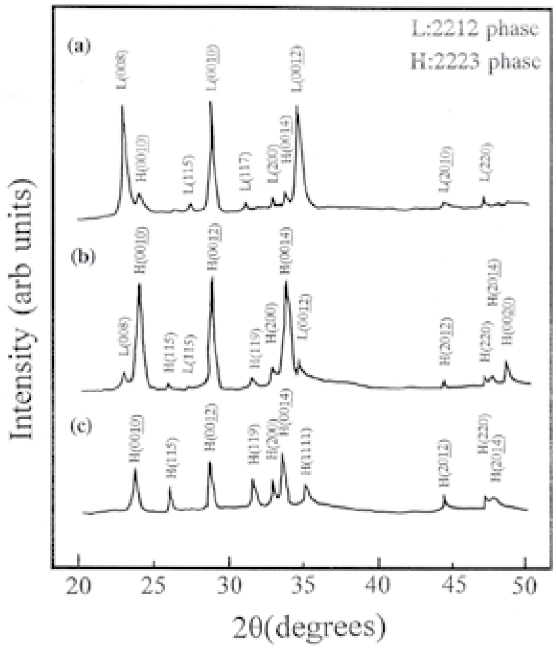


Fig.16 XRD patterns recorded from the horizontal cross-section of the sample sintered at 850℃ for 120 h with a 15℃/cm temperature gradient in 0 T magnetic field: (a) the upper sample, (b) the center of the sample, (c) the lower sample.

X-ray diffraction patterns recorded from the horizontal cross-section of the center of samples sintered at 850℃ for 120 h under different conditions are shown in Fig.17. Figure 17a is a XRD pattern on the sintering condition without temperature gradient and magnetic field, which indicates random microstructure. However, XRD patterns (Figs.17b and 17c) on the sintering condition with the temperature gradient of 15℃/cm show a strong *c*-axis alignment of Bi-2223 phase. Moreover, samples sintered in the temperature gradient and in a 10 T magnetic field have a stronger *c*-axis alignment of Bi-2223 phase than that sintered in the temperature gradient but without magnetic field. It is suggested that both the temperature gradient and magnetic field during sintering are favorable for the *c*-axis alignment of Bi-2223 phase.

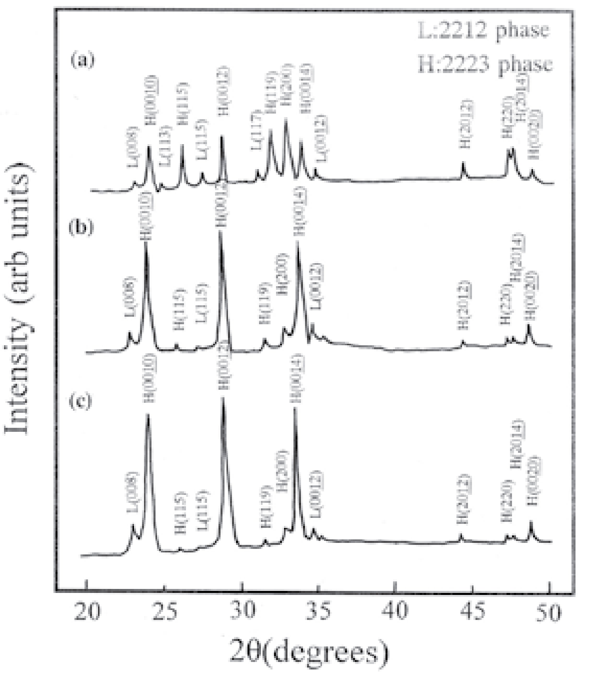


Fig.17 XRD patterns recorded from the horizontal cross- section of the center of the sample sintered at 850℃ for 120 h: (a) without temperature gradient in 0 T, (b) with a 15℃/cm temperature gradient in 0 T, (c) with a 15℃/cm temperature gradient in 10 T.

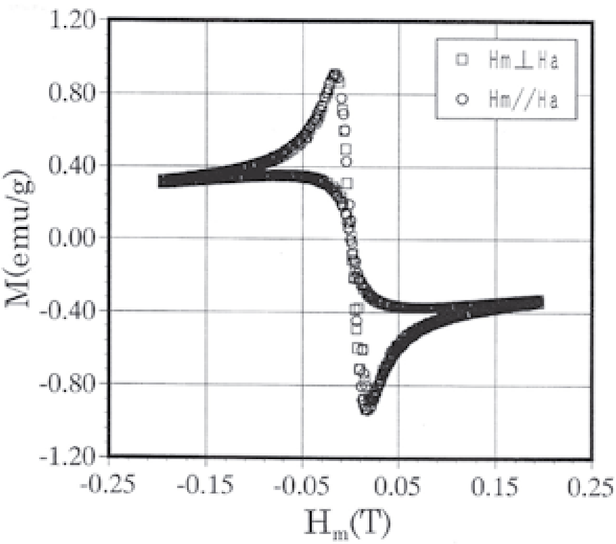


Fig.18 Magnetic hysteresis loops at 77 K for the sample sintered at 850℃ for 120 h without temperature gradient in 0 T.

Figures 18 and 19 show the measurement results obtained at 77 K for two samples sintered at 850℃ with the temperature gradient and without temperature gradient in 0 T magnetic field, respectively. The magnetic hysteresis loops in the two measuring directions are almost the same for the sample prepared without temperature gradient. Whereas for the sample sintered in 15℃/cm temperature gradient, the hysteresis in the magnetization is greater for a measuring field applied parallel to $H_a$ direction, that is $\Delta M_{Hm//Ha} > \Delta M_{Hm\perp Ha}$, indicating that for this sample an obvious anisotropy exists, and the Bi-2223 grains align with their *c*-axes parallel to $H_a$ direction.

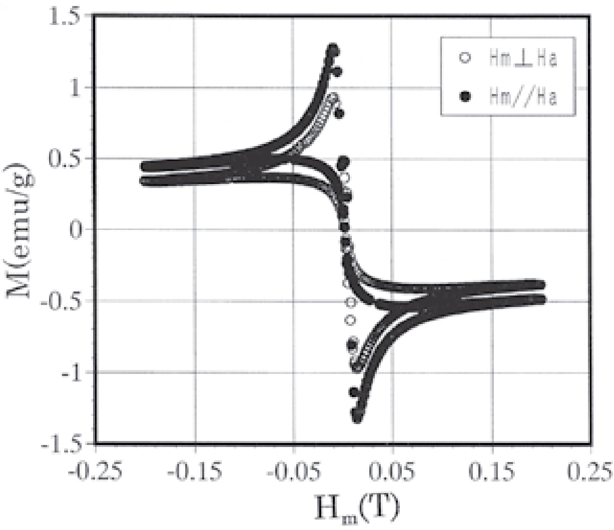


Fig.19 Magnetic hysteresis loops at 77 K for the sample sintered at 850℃ for 120 h with a 15℃/cm temperature gradient in 0 T.

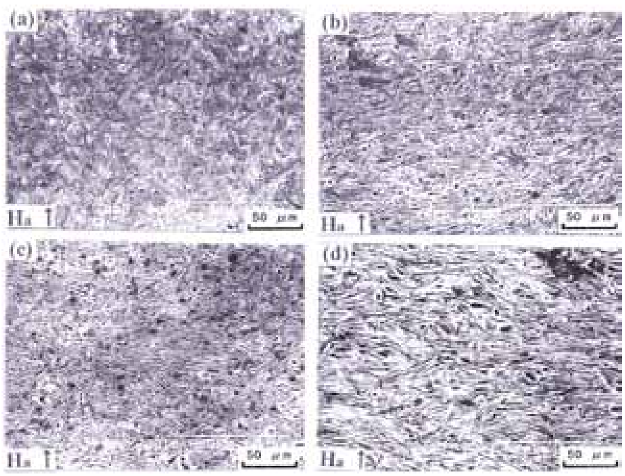


Fig.20 SEM micrographs taken from the center of the vertical section of the samples sintered at 850℃ for 120 h: (a) without temperature gradient in 0 T, (b) without temperature gradient in 10 T, (c) with a 15℃/cm temperature gradient in 0 T, (d) with a 15℃/cm temperature gradient in 10 T.

The microstructures of samples were observed by SEM on polished faces parallel to the vertical direction. Figure 20 shows SEM micrographs of the center of the vertical section of samples sintered at 850℃ for 120 h under different conditions. According to the analyses by XRD and EDS, the microstructures in these samples mainly consist of Bi-2212, Bi-2223 and Bi-free phases (including $(Sr,Ca)_2CuO_3$ and $(Sr,Ca)CuO_2$). No preferred orientation is observed in the sample sintered without temperature gradient and magnetic field (Fig.20a). In contrast, the Bi-2223 and/or Bi-2212 (grey matrix phase) are preferentially oriented perpendicular to $H_a$ direction in samples sintered in 15℃/cm temperature gradient or in 10 T magnetic field (Figs.20b, 20c and 20d).

## 4. Conclusion

The microstructure and superconducting properties of Bi-2223 superconductor fabricated in high magnetic fields were systematically investigated. The results shows that the Bi-2212 grains with their *c*-axis parallel to the magnetic field were formed after the partial-melting and solidification in 8 T magnetic field, and transformed into the Bi-2223 grains with *c*-axis alignment during the further sintering process at 840℃ without magnetic field. The conversion of Bi-2212 grains to Bi-2223 grains has the heredity in grain alignment. The mixed structures of the Bi-2223 and the Bi-2212 grains with their *c*-axis parallel to the magnetic field are formed in samples sintered at 850℃- 855℃ in 10 T magnetic field. Below 845℃ sintering in 10 T, a high proportion of Bi-2223 phase is obtained, however no preferred orientation is observed. It is suggested that a liquid phase is important for the formation of the textured structure in magnetic fields. The Bi-2223 grains with their *c*-axis parallel to the axial direction of the vertical tube furnace are formed not only on the surface, but also in the center of the sample sintered at 850℃ for 120 h in a 15℃/cm temperature gradient without magnetic field. Moreover, the samples sintered in the temperature gradient and in a 10 T magnetic field have a stronger *c*-axis alignment of Bi-2223 phase. It is suggested that both the temperature gradient and magnetic field during sintering are favorable for the *c*-axis alignment of Bi-2223 phase.

## References


(1) Maeda, H., Tanaka, Y., Fukutomi, M., Asano, T. (1988): A new high-$T_c$ oxide. superconductor without a rare earth element, *Jpn. J. Appl. Phys.*Vol. 27, pp209-215.

(2) Assmus, W., Schmidbauer, W. (1993): Crystal growth of HTSC materials, *Supercond. Sci. Technol*. Vol. 6, pp555-563.

(3) Strobel, P., Toledano, J. C., Morin, D., Schnec, J., Vacquier, G., Monnereau, O.Primot, J., Fournier, T. (1992): Phase diagram of the system $Bi_{1.6}Pb_{0.4}Sr_2CuO_6$-$CaCuO_2$ between 825°C and 1100°C, *Physica C,* Vol. 201, pp27-42.

(4) Martin, S., Fiory, A. T., Fleming, R. M., Espinosa, G. P., Cooper, A. S. (1989): Anisotropic critical current density in superconducting $Bi_2Sr_2CaCu_2O_8$ crystals, *Appl. Phys. Lett.* Vol. 54, pp72-82.

(5) Rango, P. De, Lees, M., Lejay, P., Sulpice, A., Tournier, R., Ingold, M., Germi, P., Pernet, M. (1991): Texturing of magnetic materials at high temperature by solidification in a magnetic field, *Nature* Vol. 349, pp770-772.

(6) Noudem, J. G., Beille, J., Bourgault, D., Chateigner, D., Tournier, R. (1996): Bulk Bi-Pb-Sr-Ca-Cu-O (2223) ceramics by solidification in a magnetic field, *Physica C,* Vol. 264, pp325-330.

(7) Pavard, S., Villard, C., Bourgault, D., Tournier, R. (1998): Effect of adding MgO to bulk Bi2212 melt textured in a high magnetic field, *Supercond. Sci. Technol*. Vol. 11, pp1359-1366.

(8) Mikelson A. E., Karklin, Y. K. (1981): Control of crystallization processes by magnetic fields, *J. Cryst. Growth,* Vol.52, pp524-529.

(9) Lu, X.Y., Nagata, A., Sugawara, K., Kamada S. (1999): Grain alignment and critical current densities (Bi,Pb)-2223 phase in the partial-melting and sintering process, *Supercond. Sci. Technol*. Vol. 12, pp1098-1101.

(10) Lu, X.Y., Nagata, A., Sugawara, K., Kamada S. (2000): Effect of MgO and $Ag_2O$ on the microstructure and superconducting properties of the (Bi,Pb)-2223 phase in the partial-melting and sintering process, *Physica C*, Vol. 335, pp51-55.

(11) Lu, X.Y., Nagata, A., Watanabe, K., Nojima, T., Sugawara, K., Kamada S. (2002): Crystal growth of Bi-2201 phase in high magnetic fields, *Physica C*, Vol. 382, pp27-31.

(12) Lu, X.Y., Nagata, A., Watanabe, K., Nojima, T., Sugawara, K., Kamada S. (2001): Texture and formation of (Bi,Pb)-2223 phase after partial-melting and solidification in high magnetic fields, *IEEE Transactions on Applied Superconductivity*, Vol. 11 (1), pp3553-3556.

(13) Lu, X.Y., Nagata, A., Watanabe, K., Nojima, T., Sugawara, K., Kamada S. (2002): The texture and formation of (Bi, Pb)-2223 phase with $Ag_2O$, MgO and $B_2O_3$ additions after partial-melting and solidification in high magnetic fields, *Advances in Cryogenic Engineering* (Mater.), Vol. 48, pp383-388.

(14) Lu, X.Y., Nagata, A., Watanabe, K., Nojima, T., Kamio, D., Sugawara, K., Hanada S., Kamada S. (2002): Microstructure and critical current densities of (Bi,Pb)-2223 superconductors solidified in high magnetic fields, *J. Japan Inst. Metals*, Vol. 68 (4), pp254-259.

(15) Lu, X.Y., Nagata, A., Watanabe, K., Nojima, T., Kamio, D., Sugawara, K., Hanada S., Kamada S. (2003): Formation and texture of Bi-2223 phase during sintering in high magnetic fields, *Physica C*, Vol. 392-396, pp453-457.

(16) Lu, X.Y., Nagata, A., Watanabe, K., Nojima, T., Kamio, D., Sugawara, K., Hanada S., Kamada S. (2004): Formation and texture of Bi-2223 phase during sintering in a temperature gradient, *Physica C*, Vol.412-414, pp602-606.

(17) Lu, X.Y., Nagata, A., Sugawara, K., Watanabe, K., Nojima, T. (2006): Bi-based superconductors fabricated in high magnetic fields, *Trans. Nonferrous Met. Soc. China*, Vol. 16, pp11-22.

(18) Lu, X.Y., Nagata, A., Sugawara, K., Watanabe, K., Nojima, T. (2006): Microstructure and superconducting properties of Bi-2223/Ag tapes fabricated in high magnetic fields, *Journal of Physics*: *Conference Series* Vol.51, pp287-290.

(19) Lu, X.Y., Nagata, A., Watanabe, K., Nojima, T., Chen, H. (2009): Effect of the magnetic fields on microstructure and critical current properties of the Bi-2223 tapes, *Physica C*, Vol. 469, pp1505-1508.

(20) Watanabe, K., Awaji, S., Kimura, K. (1997): Development of high field heat-treatment equipment and relevant application, *Jpn. J. Appl. Phys*. Vol. 36, pp673-675.

(21) Chen, W. P., Maeda, H., Kakimoto, K., Zhang, P. X., Watanabe, K., Motokawa, M., Kumakura, H., Itoh, K. (1999): Textured crystal growth of Bi(Pb)2212 bulk ceramics in high magnetic field, *J. Crystal Growth*, Vol. 204, pp69-75.

# 強磁場で育成した Bi 系超伝導体

魯　小葉**

強磁場で育成した Bi 系超伝導体の組織および超伝導特性について総合的に研究した。その結果、８T の強磁場中における半溶融・凝固した試料の水平面では磁場付加方向に c 軸配向する Bi-2212 相の組織を確認することができる。さらに、無磁場 840℃で焼結すると、水平面の c 軸配向した Bi-2212 相は c 軸配向した Bi-2223 相になる。Bi-2212 相から Bi-2223 相への相変態では、Bi-2212 相が配向していれば、その後の相変態によって生成する Bi-2223 相も c 軸配向する。10T の強磁場における 850℃~855℃温度範囲で焼結した試料では c 軸配向した Bi-2212 相と Bi-2223 相の混合組織が観察された。10T で 845℃以下の温度で焼結した試料では、Bi-2223 相の生成率が高いが、c 軸配向性はなかった。無磁場で 15℃/cm の温度勾配下で焼結した試料では c 軸配向した Bi-2223 相の組織を示した。さらに、10T の強磁場を印加した場合には、Bi-2223 相の配向度が高くなることが分かった。

**秋田大学大学院工学資源研究科共同ライフサイクルデザイン工学専攻